SCIENCE CHINA
Technological Sciences

• Article •

June 2017 Vol.60 No.6: 893–901
doi: 10.1007/s11431-016-0220-1

Free-surface air entrainment in open-channel flows

WEI WangRu, XU WeiLin, DENG Jun*, TIAN Zhong & ZHANG FaXing

State Key Laboratory of Hydraulics and Mountain River Engineering, Sichuan University, Chengdu 610065, China

Received March 23, 2016; accepted September 18, 2016; published online October 31, 2016

In hydraulic engineering, free-surface aeration is a natural phenomenon occurring in smooth channel flows. In self-aerated flows, a key aspect that has not yet been well understood is the formation mechanism of free-surface air entrainment. In this research, the process of free-surface entrapped deformation is analyzed theoretically and the critical radius of curvature for air entrainment is obtained, affected by flow mean velocity and depth. When the severity of local free-surface deformation exceeds the critical condition, the entrapped free surface encounters closure in the unstable deformation movement process, resulting in air entrainment. This inference agrees well with observed experimental results that are obtained from the processes of surface entrapped deformation and air entrainment captured by a high-speed camera-based data acquisition system. This agreement indicates that self-aeration occurs in low-velocity open-channel flows. It is also confirmed that free-surface turbulent deformation provides a mechanism for air entrainment.

hydraulic engineering, self-aeration, turbulence, free surface, open-channel flows

Citation: Wei W R, Xu W L, Deng J, et al. Free-surface air entrainment in open-channel flows. Sci China Tech Sci, 2016, 60: 893–901, doi: 10.1007/s11431-016-0220-1

1 Introduction

Steep chutes and spillways are of great importance in the design of hydraulic structures. Under certain conditions in such chutes and spillways, a large amount of air can be entrained through a free surface into the water in high-velocity flows. In self-aerated open-channel or chute flows, a key aspect that has not yet been well understood is the formation mechanism of air entrainment [1,2]. It is well known that self-aeration is caused by the interaction between a turbulent boundary layer and free surface [3–5]. Traditionally, it is believed that the inception of air entrainment occurs as soon as the turbulence development reaches the free surface. However, this is the necessary condition for air entrainment [6]; the sufficient condition is that the eddy turbulence intensity should exceed a certain threshold [7]. This condition must be relevant to the microscopic deformation movement on the free surface of water. However, there is a lack of understanding regarding this process.

Traditional studies note that 'air bubbles can be entrained into a flow when drops led by a breakup of liquid masses fall back into the bulk liquid in the end and bubbles pulled into the water are transported along with the air-water flow'. Studies on drop impact have shown that drop impact indeed causes the entrainment of bubbles [8,9]. Researchers studied the impact of drops on stationary and fluid liquid surfaces [10–13]. The results showed that the critical conditions for the drop size and impact velocity are strict and that the amount of entrained air bubbles is smaller in a flowing liquid than in a stationary liquid. Based on these studies, critical conditions for the onset of self-aeration and the formation of drops have been established.

However, self-aeration also occurs when the flow velocity is so low that the turbulence intensities are not sufficiently high to cause drops to eject out of the bulk liquid

*Corresponding author (email: djhao2002@scu.edu.cn)

and entrained air [14,15]. This indicates that drop impacts are not the only process of entraining air. Falvey and Ervine [16] considered the formation of bubbles caused by distorted free-surface closure; the mechanism they proposed explains the air bubble entrainment at flow velocities smaller than the critical value required for the formation of air-entraining drops, but the relationship between free-surface deformation and air entrainment is still not very clear. In addition, considering the random direction of turbulent movement, it is necessary to treat the entrapped free-surface roughness and the breakup liquid mass equally, and both these processes happen simultaneously. The dynamic and kinematic processes at free surfaces play important roles in the case of free-surface deformation affected by turbulence intensity [17,18]. However, the research conducted on this topic is insufficient and only little is known about the characteristic features of such flows.

The objective of this research is to present a simple two-dimensional model of free-surface deformation based on dynamic and energy transitions, with the aim to describe the relationship between free-surface entrapped deformation and air entrainment. A microscopic sufficient condition for surface air entrainment is developed. Moreover, the free-surface deformation and air bubble entrainment processes in high-speed open-channel flows is studied using a high-speed video system to capture associated events in detail. The theoretical model-based analysis is applicable to the visual process of air entrainment caused by free-surface turbulent movement. This study therefore gives further insight into the structure of free-surface turbulence in high-speed velocity flows.

2 Advances in study of air entrainment mechanism

Rein [19] analysed the mechanism of air entrainment due to drops falling back into the bulk flow, following the classical approach of Davies [20] based on dynamic and kinematic processes. A critical condition is obtained: a drop that is projected from the bulk flow and that contributes to air entrainment will separate only if the maximum height of its trajectory exceeds its radius. The maximum height of a drop depends on the velocity and depth of the open-channel flow. This is a typical description of free-surface deformation for self-aeration.

Based on the critical condition for drop generation and self-aeration, Rein [19] compared actual drops with free-surface drop shapes obtained from previously photographs in self-aerated open-channel flows. The comparison showed that the conventional concepts of drop formation are inadequate to explain the ejection of drops to heights observed in experiments and that the energy of the ejected drops is not sufficiently high for air entrainment, implying that drop impacts are not the only process of entraining air.

High-speed stop-action photographs taken during flume experiments showed that the free surface of water remains intact but very contorted with a very small quantity of flying droplets over the free surface of the self-aerated open-channel flow at high velocities and air content [21,22]. Further, based on the air-water structure of self-aerated flow, a new concept of entrapped air, which represents the air entrapped between gaps created by surface roughness, was developed to distinguish the air from the entrained air bubbles. Now, the aim is to further explore the relationship between free-surface entrapped deformation and self-aeration both theoretically and experimentally.

3 Free-surface entrapped deformation process

3.1 Critical condition

Considering a small element entrapped deformation on a free surface caused by a characterised eddy with the instantaneous vertical fluctuation velocity (v') in turbulent open-channel flows, the two-dimensional model for this process is generalised as shown in Figure 1. With the development of entrapped deformation, the roughness becomes larger and deeper. When the kinetic energy of the eddy E_e exceeds the surface energy E_σ, the free surface will become unstable. This instability is asymmetrical and disordered, and during this process, the entrapped deformed free surface can move transversely under horizontal fluctuation velocities (v_1', v_2'). When the two sides of the free surface achieve closure in the opposite direction, air bubble entrainment occurs and self-aeration is generated in the open-channel flow.

When E_e and E_σ are equal, which can be considered as a critical condition for air entrainment, an energy balance that relates E_e and E_σ has to be accounted for:

$$E_e = E_\sigma. \tag{1}$$

The turbulent kinetic and surface energies can be computed by [19, 23]

$$E_e = \frac{1}{2}\cdot\rho\cdot\frac{4}{3}\pi\left(\frac{D}{2}\right)^3\cdot v'^2, \tag{2}$$

$$E_\sigma = \pi r_C^{\,2}\cdot\sigma, \tag{3}$$

where v' is the fluctuation velocity of the eddy in the y direction, σ is the surface tension, and ρ is the water density.

D is the characteristic size of the turbulent eddy. Brocchini and Peregrine [24] analysed the turbulent eddy size that is able to disturb the surface with the energy of surface deformation. Considering the gravity ($0.13gD$) and surface tension ($1.57\sigma/\rho D$) effects, they suggested the following relationship between D and local typical velocity v^*:

$$v_*^{\,2} \approx 0.13gD + \frac{1.57\sigma}{\rho D}. \tag{4}$$

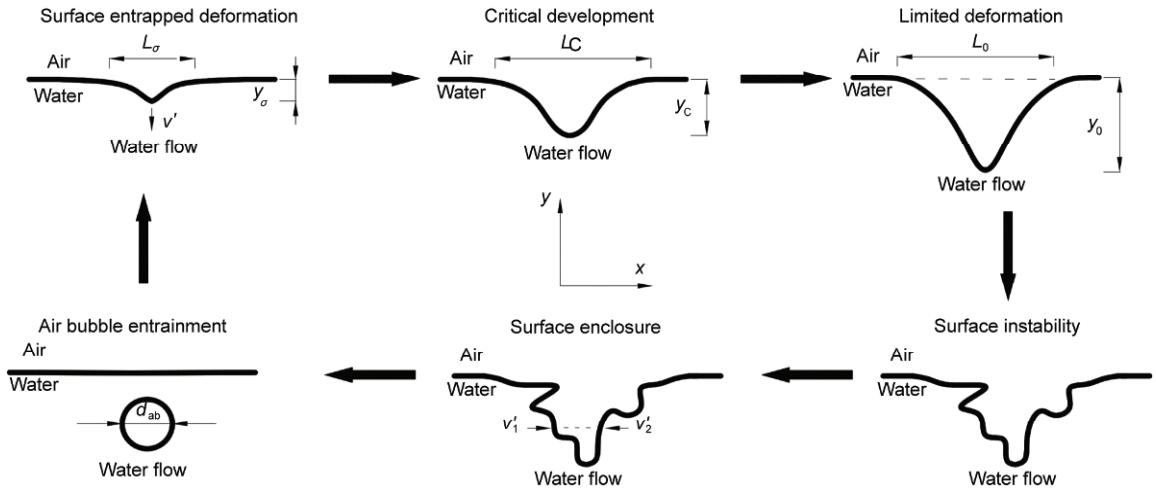

Figure 1 Sketch process of free surface deformation and air entrainment.

In the present study, the local typical velocity v^* is assumed to be the friction velocity v_τ, and before the surface entrapped deformation occurs, the surface tension effect on the instantaneous turbulent eddy size is neglected, that is, $v^{*2} \approx 0.13gD$.

In eq. (3), r_C is the radius of curvature at the apex of the deformed free-surface profile, which represents the severity of surface deformation. The surface deforms more severely for a smaller radius of curvature. Based on the above analysis, the condition for the critical radius of curvature r_C that would result in air entrainment caused by entrapped surface deformation (eq. (1)) becomes

$$r_C = \left(\frac{\rho D^3 v'^2}{12\sigma} \right)^{\frac{1}{2}}. \tag{5}$$

When the actual local r_0 of the free-surface entrapped deformation is smaller than the critical r_C ($r_0 < r_C$), the deformation severity becomes greater and the turbulent level caused by the eddy is large enough to overcome surface tension effects. Under this situation, the free surface will become unstable and will loosen. During this process, the free surface can achieve closure under the fluctuation effect, and the air entrapped in the free surface will be entrained into the water flow in the form of individual bubbles. When $r_0 > r_C$, the local surface deformation is less severe and the surface tension can overcome the turbulent fluctuation pressure and the deformed free surface can remain stable. Under this situation, the entrapped air will not be entrained into the water flow. Consequently, the actual surface deformation caused by the turbulent eddy has an important effect on the air entrainment.

3.2 Theoretical limiting condition for free-surface deformation

Under the ideal condition that the surface tension can overcome any turbulence level and the entrapped surface is stable under constant pressure fluctuation p' in the process of deformation, there will always exist a state where the surface deformation is balanced. At the instant of maximum deflection, p' is balanced by the surface tension pressure $2\sigma/r_m$ and the hydrostatic pressure $y_m\rho g$, and y_m is the maximum depth to which free-surface deformation develops. Davies [20] related pressure fluctuations in the free-surface zone to the square of the friction velocity v_τ, $p' = C_1\rho v_\tau^2$. A hydrostatic force balance at the apex of the entrapped surface yields

$$C_1\rho v_\tau^2 = \frac{2\sigma}{r_m} + y_m\rho g. \tag{6}$$

The relationship is proved correct when C_1 is of the first order, and the relationships for $v_\tau = v'$ and $C_1 = 1$ are verified a posteriori. In the free-surface region with the mean flow velocity V, an upper limit of friction velocity v_τ is determined from the relationship between V and v_τ according to the law of the wall [25]:

$$\frac{V}{v_\tau} = \frac{1}{\kappa}\ln\frac{Hv_\tau}{\nu} + B, \tag{7}$$

where κ is the Von Karman constant (0.4) and B is a constant (5.2). Previous theories and experiments about free-surface fluctuation are studied [26,27], and the value y_m is estimated as

$$y_m \approx \frac{K}{g}, \tag{8}$$

where K is the mean kinetic energy at the free surface, which is nearly equal to one half of the square of the fluctuation velocity v'. Therefore, the interaction of the turbulent eddy and free surface results in the formation of a radius of curvature that is suitable for the ideal condition:

$$r_{\mathrm{m}} = \frac{4\sigma}{\rho v'^2}. \tag{9}$$

This is the most severe deformation of the free surface without instability and air entrainment under a certain turbulence condition. Comparing eq. (5) with eq. (9), the critical condition for air entrainment through free-surface entrapped deformation is obtained as

$$r_{\mathrm{m}} \leqslant r_{\mathrm{C}}. \tag{10}$$

The results are twofold: 1) the free-surface entrapped deformation depends on the flow mean velocity and water depth and 2) air entrainment occurs only if the flow condition exceeds a threshold, as shown in Figure 2.

Figure 3 shows the effects of V and H on both the critical deformation r_{C} (eq. (5)) and ideal deformation r_{m} (eq. (9)). r_{C} and r_{m} are normalised by the water depth H relative to the entrapped deformation radius of curvature.

First, note that with an increase in the mean flow velocity V and water depth H, the value of r_{m}/H decreases, and this indicates that the ideal severity of entrapped deformation that can be achieved by the free surface becomes more intensive. Considering r_{m} to be the surface shape, the free-surface roughness becomes increasingly pronounced with V and H.

When critical severity of entrapped deformation is achieved, if V is small, r_{C}/H also becomes small, and air entrainment caused by surface entrapped closure occurs under the turbulence effect only if the severity of the free-surface entrapped deformation is quite large. With an increase in V, the critical deformation condition for air entrainment becomes less severe. This is mainly because a higher turbulence intensity makes it easier for the free surface to achieve closure, and the level of surface deformation required for air entrainment decreases compared with the case when the turbulence intensity is low. With an increase in the water depth for identical V, r_{C}/H decreases, indicating that the air entrainment condition through free-surface entrapped deformation becomes more critical for larger water depths.

The intersection point of each two-curve set (Figure 3) is the critical condition for air entrainment through free-surface entrapped deformation. When the r_{m}/H curve is above the r_{C}/H curve ($r_{\mathrm{m}}/H > r_{\mathrm{C}}/H$), the severity of free-surface deformation cannot reach the critical deformation condition and air entrainment will not occur. When the r_{m}/H curve is below the r_{C}/H curve ($r_{\mathrm{m}}/H < r_{\mathrm{C}}/H$), the severity of free-surface deformation can exceed the critical condition and self-aeration occurs. The critical velocity V_{C} for $r_{\mathrm{m}}/H = r_{\mathrm{C}}/H$ is shown in Figure 4. With an increase in the water depth, the critical velocity increases. The effect of the water depth on both r_{C} and V_{C} agrees with the phenomenon that the inception of self-aeration in an open channel is located further along the downstream with an increase in the water depth [28,29]. The relationship is approximately represented as

$$\frac{V_{\mathrm{C}}^2}{2g} = 1.4 \cdot H^{1.8}. \tag{11}$$

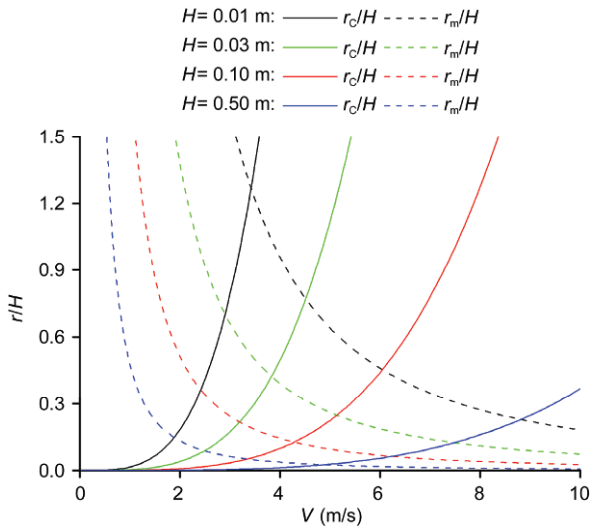

Figure 3 Relationship between flow conditions and free surface deformation.

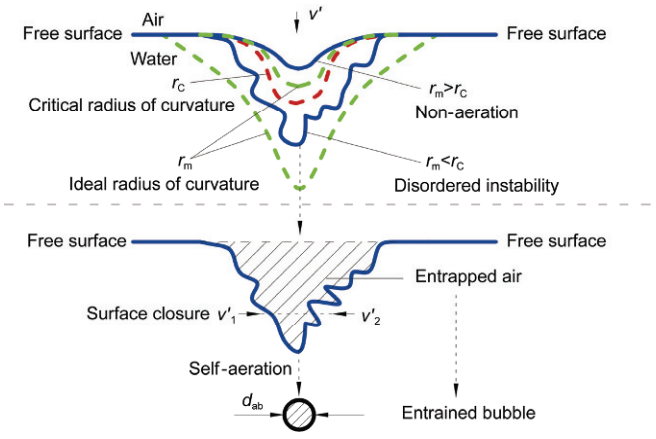

Figure 2 Comparison of r_{C} and r_{m} in free surface air entrainment.

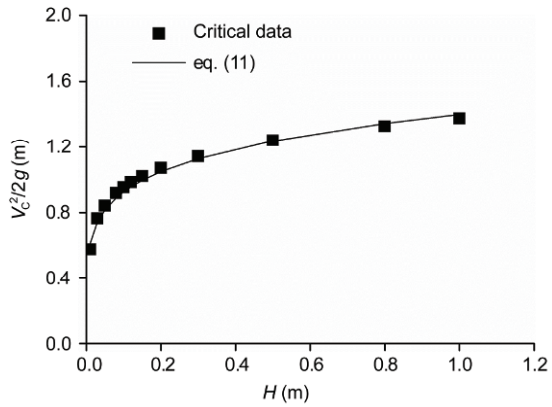

Figure 4 Critical flow velocity of air entrainment from $r_{\mathrm{C}} = r_{\mathrm{m}}$.

Based on the present analysis, V_C is approximately 3–5 m/s for H = 0.01–1 m. This result indicates that air entrainment occurs at low velocities of water flow, which is agreement with the previous experimental observations [30–32], whereas the conventional theories about drop impacts and wave breaks estimated that the critical velocity for self-aeration is larger than 5 m/s.

4 Experimental observations

Experiments are performed in a flat chute, which is 18 m long and 0.3 m wide and has a channel slope α = 28°, as shown in Figure 5. It is made of planed glass boards, and the sidewalls are 0.3 m high. Water is supplied through a closed-circuit system, which includes a flume, large tank below the chute, and pressure head tank. The water pump is controlled electronically, thus providing a fine discharge and facilitating the adjustment of the flow velocity of the approaching water. The water flows to the flume through a smooth convergent nozzle, and the exit is 0.12 m high and 0.3 m wide. The convergent nozzle is adjusted and is sufficiently long to ensure that the water is calm and flows to the chute with little disturbance (i.e., with a smooth free surface).

Free-surface deformation and air entrainment occur very rapidly, in the order of 10 ms, and a high-speed camera-based data acquisition system is always used to study surface roughness characteristics [33]. In the present study, a high-speed camera system is used to capture and present the entire process of free-surface entrapped deformation and air entrainment. The system includes a high-speed video camera (Motion Pro Y3-Classic, Integrated Design Tools Inc., USA), a Nikkor lens, an adjustment-fixing mechanism, and a computer. High-speed cinematic results are obtained for a 1280 × 504 pixel region at 6000 frame/s with an exposure time of 1.7 μs. A set of LED lights is placed opposite the flume as an artificial supplementary light source to improve image quality. The shooting scope is 40 × 12 cm^2, and the shooting position is close to the nozzle exit (approximately 0.5 m away). The velocity at the shooting position is obtained by using the discharge per unit width and the initial water depth at the nozzle exit (0.12 m). To achieve accurate free-surface deformation, the lens is adjusted to the same elevation as the free surface of water flow and controlled perpendicular to the sidewall of the flume. To reduce the sidewall effect, the focusing plane is set at the central longitudinal plane during the shooting period, and the surface deformation is considered to be mainly the result of water turbulence.

Figure 6 shows the processes of free-surface deformation and air entrainment at flow velocity V = 7.6 m/s. Because of the interaction of the surface tension and sidewall effect, the water profile near the sidewall is higher than the central water profile. The free-surface roughness and the development of free-surface deformation into the flow can be clearly seen. In the size analysis of surface deformation, the free-surface position is the local average position from both the sides of the entrapped area. A distinctive surface air trough is entrapped in the water, resulting in a longitudinal vortex (Figure 6(a), t = 0.004 s; Figure 6(b), t = 0.003 s), and air is finally entrained and detained by the main flow as bubbles (Figure 6(a), t = 0.026 s; Figure 6(b), t = 0.011 s). A cycle duration is typically 10^{-2} s for the present visual observation, and it is uncertain as to what extent this cycle duration can be applied to other conditions. The free-surface entrapped deformation and air entrainment processes are schematically shown in Figure 7, as interpreted from Figure 6.

As shown in Figure 8(a), at the original time (t = 0.000 s),

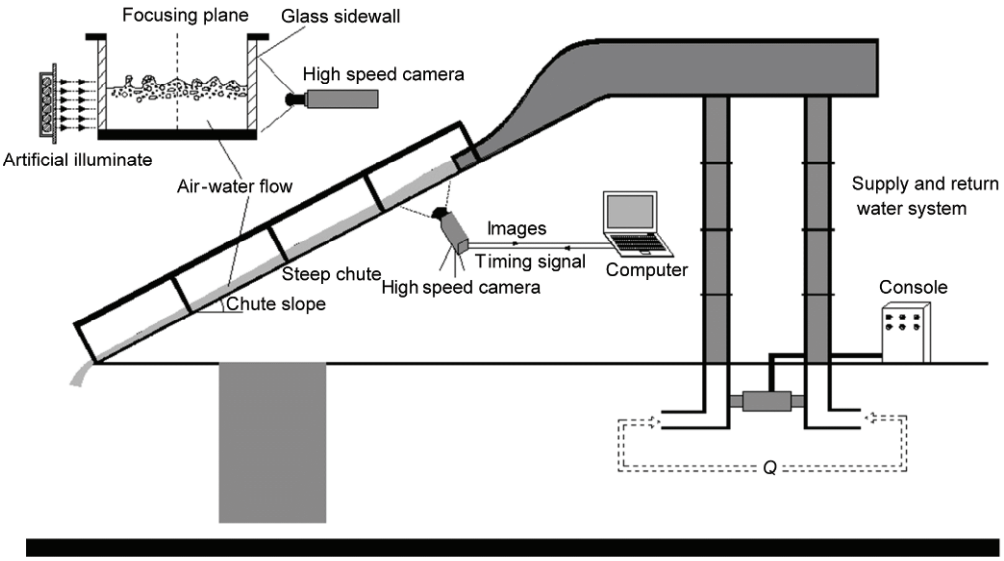

Figure 5 Schematic of experimental channel and high-speed camera acquisition system.

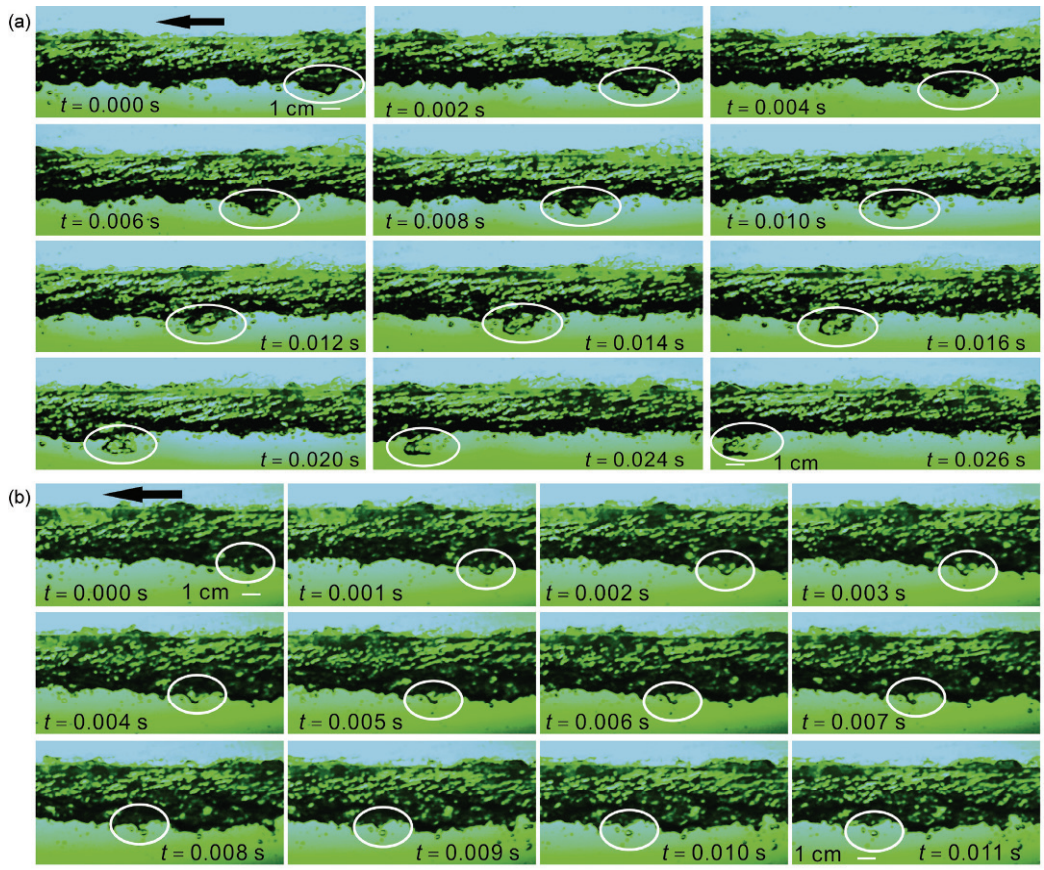

Figure 6 Processes of surface deformation and air entrainment: (a) Large bubble entrainment (d_{ab} = 12.4 mm); (b) small bubble entrainment (d_{ab} = 4.2 mm).

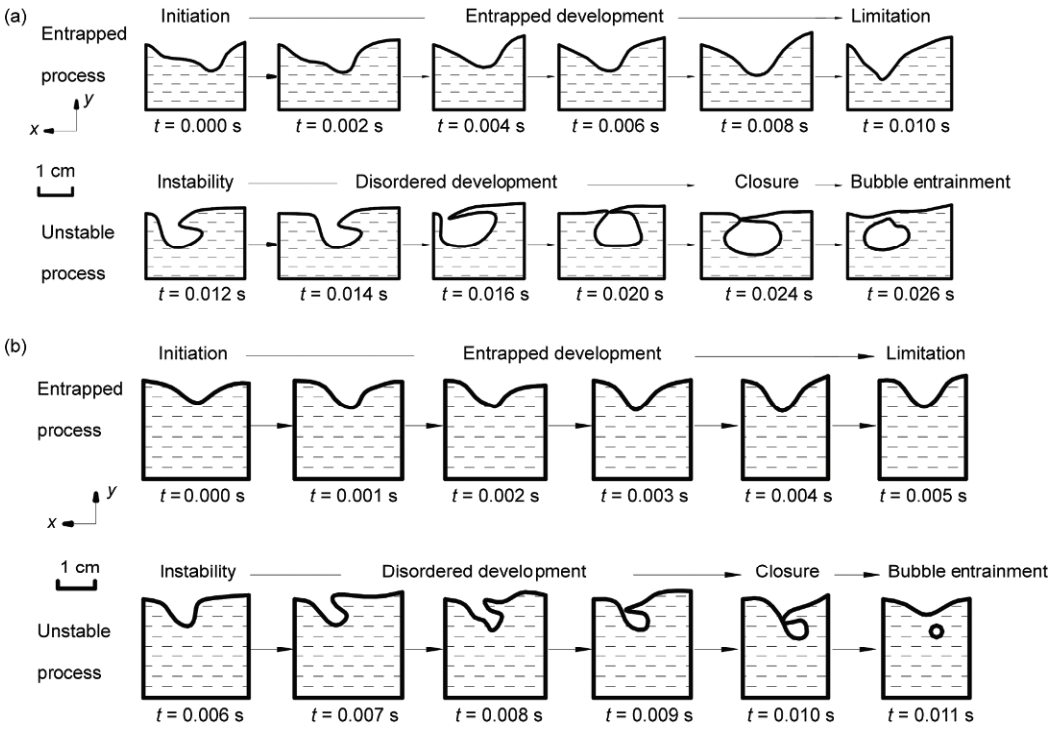

Figure 7 Sketch of free surface movement and air entrainment: (a) Large bubble entrainment (d_{ab} = 12.4 mm, Figure 6(a)); (b) small bubble entrainment (d_{ab} = 4.2 mm, Figure 6(b)).

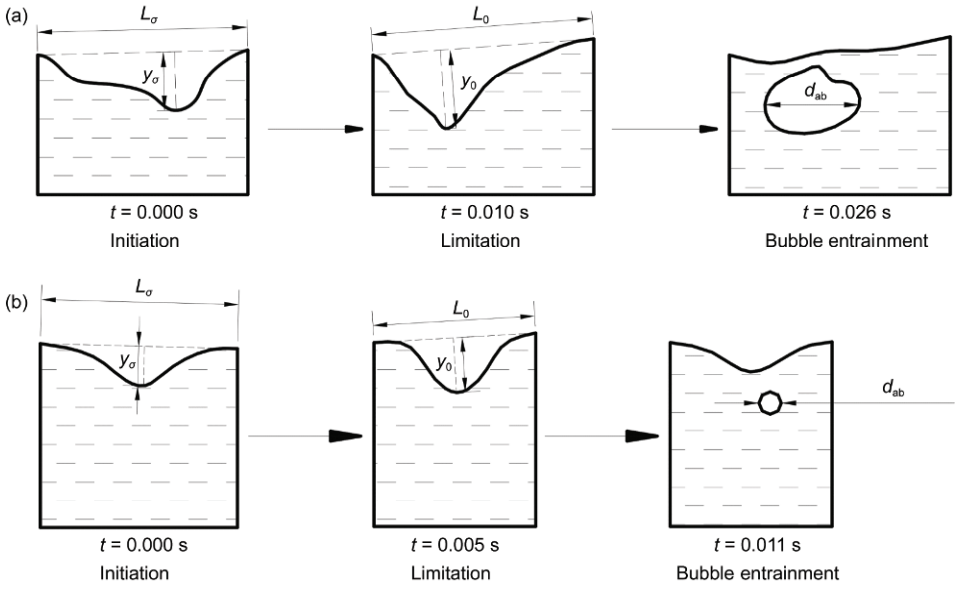

Figure 8 Key periods of free surface deformation and air entrainment: (a) Large bubble entrainment (d_{ab} = 12.4 mm, Figure 6(a)); (b) small bubble entrainment (d_{ab} = 4.2 mm, Figure 6(b)).

there is a clear 'hollow' entrapped in the water flow; the free surface on both the sides are higher than the entrapped centre, and the size of the small free-surface roughness is L_σ = 30.2 mm and y_σ = 8.7 mm. At t = 0.010 s, with the development of the entrapped 'hollow', the free surface becomes stable, the apex develops deeper into the flow, and the apex width becomes larger with L_0 = 41.5 mm and y_0 = 12.1 mm. Then, at t = 0.010–0.020 s, the free surface is unstable and becomes loose. It can be seen that the free surface achieves closure from t = 0.020~0.026 s, and an air bubble is entrained into the flow with d_{ab} = 12.4 mm (t = 0.026 s, along the x direction). For relatively small air bubble entrainment (d_{ab} = 4.2 mm, Figure 8(b)), the entire process is similar to the one described above and the free surface achieves closure at a relatively low position.

The simple two-dimensional theoretical analysis results are in good agreement with the experimental observations in terms of the free-surface deformation and air entrainment processes, and the free-surface roughness plays an important role in helping us understand the formation of self-aerated air-water flows. The surface entrapped deformation can be assumed to be a Gaussian-curve-type deformation and can be well approximated like the surface ejection deformation [19,20]; r is given by

$$r = \frac{L^2}{8y}, \tag{12}$$

where L is the width of the curve and y is the maximum deflection, as shown in Figure 1. Detailed experimental data on the free-surface deformation are obtained, as shown in Figure 9. The radius of curvature centralises between the critical condition r_C and ideal condition r_m when the

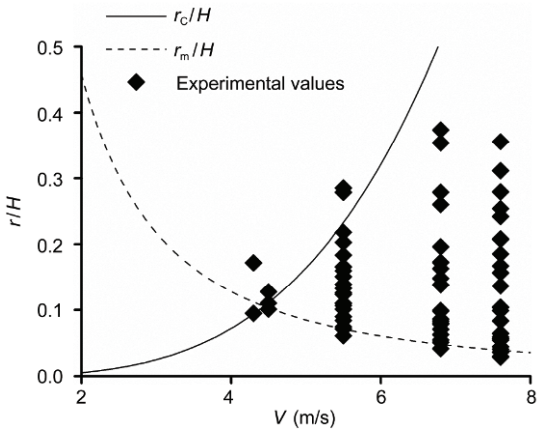

Figure 9 Comparison of experimental and theoretical values (H = 0.12 m).

entrapped free surface becomes unstable initially. This indicates that the free-surface deformation severity in experiments exceeds the critical condition when surface instability occurs; however, it cannot reach the ideal maximum deformation severity because the surface tension cannot balance the greater turbulence effect.

Two key issues are involved in the formation of self-aerated air-water flow: (1) penetration of air into the free surface of water, that is, the air entrainment mechanism and (2) existence of air in the flow, that is, the air diffusion capacity. The present study shows the mechanism of free-surface air entrainment; that is, when the free-surface deformation exceeds the critical form condition, air will be entrained into the water during the process of free-surface instability. In addition, various macro-scale flow characteristics cause the free-surface deformation. The high local

turbulence intensity of the free surface can be improved by water drop impact, free-surface roughness caused by a solid surface such as a stepped and rocked chute, and narrow-deep flow that is affected by the side solid surface, except for the main flow mean velocity [34,35]. Although clear similarities have been observed in such self-aerated flows over smooth and stepped chutes, some distinctive features have been reported in many studies [36–39]. The air diffusion in water flow is controlled by a process of air transport, which is affected by the mean turbulence intensity and buoyancy of water. Further studies on aerated air-water flow should focus on analyzing the tiny-scale surface form feature and the influence of air entrainment mechanism on self-aeration scale effect.

5 Conclusions

In this study, based on a simple two-dimensional model of free-surface deformation, the process of entrapped deformation and air entrainment is analyzed and a critical radius of curvature of the free surface is developed for the formation of self-aeration. The critical condition of free-surface entrapped deformation depends on the flow mean velocity and water depth, and air will be entrained into the water during the process of free-surface instability when local radius of curvature exceeds the critical condition. The theoretical analysis results are in good agreement with the results of the observed air entrainment process. This indicates that free-surface entrapped deformation caused by turbulence is a possible mechanism by which self-aeration occurs in open-channel flows. Based on the present theoretical analysis, the critical velocity of air entrainment is found to be approximately 3–5 m/s for a wide range of flow depths 0.01–1 m. This result indicates that air entrainment and self-aeration can occur in low-velocity open-channel flows. Further studies on aerated air-water flow should focus on analysing the tiny-scale surface form feature and the influence of air entrainment mechanism on self-aeration scale effect.

The work was supported by the National Natural Science Foundation of China (Grant No. 51379138) and the National Basic Research Program of China ("973" Project) (Grant No. 2013CB035905).

1 Wood I R, Ackers D, Loveless J. General method for critical point on spillways. J Hydraul Eng, 1983, 109: 308–312
2 Anwar H O. Self-aerated flows on chutes and spillways-Discussion. J Hydraul Eng, 1994, 120: 778–779
3 Lane E W. Entrainment of air in the swiftly flowing water. Civ Engrg, 1939, 9: 89–91
4 Chanson H. Turbulent air-water flows in hydraulic structures: Dynamic similarity and scale effects. Chem Eng Res Des, 2009, 87: 789–797
5 Felder S, Chanson H. Free-surface profiles, velocity and pressure distributions on a broad-crested weir: A physical study. J Irrigation Drainage Eng ASCE, 2012, 138: 1068–1074
6 Wu C G. Air-Water Two-Phase Flows in Open Channel (in Chinese). Chengdu: Chengdu University of Science and Technology Press, 1998
7 Chanson H. Self-aerated flows on chutes and spillways. J Hydraul Eng, 1993, 119: 220–243
8 Rein M. Phenomena of liquid drop impact on solid and liquid surfaces. Fluid Dyn Res, 1993, 12: 61–93
9 Rein M. The transitional regime between coalescing and splashing drops. J Fluid Mech, 1996, 306: 145–165
10 Pumphrey H C, Bjørnøl C L A. Underwater sound produced by individual drop impacts and rainfall. J Acoust Soc Amer, 1989, 85: 1518–1526
11 Oguz H N, Prosperetti A. Bubble entrainment by the impact of drops onliquid surfaces. J Fluid Mech, 1990, 219: 143–179
12 Medwin H, Kurgan A, Nystuen J A. Impact and bubble sound form raindrops at normal and oblique incidence. J Acoust Soc Amer, 1990, 88: 413–418
13 Cole D E, Liow J L. Bubble entrapment during water drop impacts. In: Proceedings of the 15th Australasian Fluid Mechanics Conference. Sydney: The University of Sydney, 2004
14 Straub L G, Anderson A G. Experiments on self-aerated flow in open channels. J Hydraul Div, ASCE, 1958, 84: 1–35
15 Volkart P. The mechanism of air bubble entrainment in self-aerated flow. Int J Multiphase Flow, 1980, 6: 411–423
16 Falvey H T, Ervine D A. Aeration in jets and high velocity flows. In: Proceedings of the International Symposium, Model-Prototype Correlation of Hydraulic Structures. New York: Hydraulics division of the ASCE, 1988
17 Nezu I, Nakagawa H. Turbulence in Open-Channel Flows. Rotterdam: IAHR monograph, Bulkema Publishers, 1993
18 Banerjee S. Upwellings, downdrafts, and whirlpools: Dominant structures in free surface turbulence. Appl Mech Rev, 1994, 47: 166–172
19 Rein M. Turbulent open-channel flows: Drop-generation and self-aeration. J Hydraul Eng, 1998, 124: 98–102
20 Davies J T. Turbulence Phenomena. New York: Academic Press, 1972
21 Killen J M. The surface characteristics of self-aerated flow in steep channels. PhD Thesis. Minneapolis: University of Minnesota, 1968
22 Wilhelms S C, Gulliver J S. Bubbles and waves description of self-aerated spillway flow. J Hydraul Res, 2005, 43: 522–531
23 Wu C G. A research on self-aerated flow in open channels (in Chinese). J Hydroel Eng, 1998, 23: 23–36
24 Brocchini M, Peregrine D H. The dynamics of strong turbulence at free surfaces, Part 1: Description. J Fluid Mech, 2001, 449: 225–254
25 Pope S B. Turbulent Flows. Cambridge: Cambridge University Press, 2000
26 Borue V, Orszag S A, Staroselsky I. Interaction of surface waves with turbulence: Direct numerical simulations of turbulent open-channel flow. J Fluid Mech, 1995, 286: 1–23
27 Nakayama A, Yokojima S. Modeling free-surface fluctuation effects for calculation of turbulent open-channel flows. Environ Fluid Mech, 2003, 3: 1–21
28 Michels V, Lovely M. Some prototype observations of air entrained flow. In: Proceedings of Minnesota International Hydraulics Convention. Minneapolis: University of Minnesota, 1953
29 Ferrando A M, Rico J R. On the incipient aerated flow in chutes and spillways. J Hydraul Res, 2002, 40: 95–97
30 Hall L S. Open channel flow at high velocities. Trans ASCE, 1943, 108: 1394–1434
31 Chanson H. Air bubble entrainment in open channels: Flow structure and bubble size distributions. Int J Multiphase Flow, 1997, 23: 193–203
32 Zhang F X, Xu W L, Zhu Y Q. Experimental study on formation of

air bubbles in self-aerated open channel flows (in Chinese). J Hydraul Eng, 2010, 41: 343–347
33 Bung D B. Non-intrusive detection of air-water surface roughness in self-aerated chute flows. J Hydraul Res, 2013, 51: 322–329
34 Pagliara S, Carnacina I, Roshni T. Inception point and air entrainment on flows under macroroughness condition. J Environ Eng ASCE, 2011, 137: 629–638
35 Pfister M, Hager W H. Self-entrainment of air on stepped spillways. Int J Multiphase Flow, 2011, 37: 99–107
36 Meireles I, Matos J. Skimming flow in the non-aerated region of stepped spillways over embankment dams. J Hydraul Eng, 2009, 135: 685–689
37 Meireles I, Renna F, Matos J, et al. Skimming, nonaerated flow on stepped spillways over roller compacted concrete dams. J Hydraul Eng, 2012, 138: 870–877
38 Matos J, Meireles I. Hydraulics of stepped weirs and dam spillways: Engineering challenges, labyrinths of research. In: Proceedings of 5th International Symposium on Hydraulic Structures. Brisbane: The University of Queensland, 2014
39 Xu W L, Luo S J, Zheng Q W, et al. Experimental study on pressure and aeration characteristics in stepped chute flows. Sci China Tech Sci, 2015, 58: 720–726